Effects of Viscous Dissipation and Heat Generation on Free Convection Flow along A Vertical Flat Plate with Variable Viscosity and Thermal Conductivity

Sree Pradip Kumer Sarker[1*], Sirazum Munira[2], Md. M. Alam[3]
[1] *Ph.D. Researcher, Dhaka University of Engineering & Technology, Gazipur, Bangladesh.*
[2]*Ph.D. Researcher, Dhaka University of Engineering & Technology, Gazipur, Bangladesh.*
[3]*Professor, Department of Mathematics, Dhaka University of Engineering & Technology, Gazipur, Bangladesh.*

Abstract: Natural convection over a vertical plate heated in the presence of variable viscosity and thermal conductivity is of great importance from an engineering point of view, and many researchers have studied this topic. The nature of heat generation and viscous dissipation on natural convection flow along a vertical flat plate is investigated in this work. Two-dimensional laminar flow and unstable boundary layer equations are discussed here. The fundamental governing equation is turned into a dimensionless governing equation by using the necessary variables. The Crank Nicolson scheme is an efficient implicit finite difference approach for numerical computations of these equations. Heat generation, viscosity dissipation and thermal conductivity were explored in this work. The impacts of numerous parameters are demonstrated in this study and compared to other researchers' velocity profiles, temperature profiles, local skin friction, and local heat transfer coefficient. Compare the present numerical results to the work outcomes that were previously released. It also compares the number of works available to the number of works published previously. The results are given in both figures and tables for various values of related physical parameters.

Keywords: Heat Generation, Viscous Dissipation, Variable Viscosity, Dependent Thermal Conductivity.

I. Introduction

Natural convection occurs as the fluid's density varies as a result of temperature changes. Because of its widespread usage in both science and engineering, natural convection has piqued the interest of many academics. In addition, scientists and academics are fascinated by the topic of natural convection flow down a vertical flat plate because of the several applications it may potentially serve. This phenomenon is widely seen in the design of micro structures and fluid flows around shrouded heat dissipation fins in a variety of technical applications such as cooling molten metal and nuclear reactors. When it comes to industrial cooling, natural convection is a popular method. The resistance to the flow of fluid is measured by viscosity, which is also a measure of internal fluid friction. To dissipate energy, labor must be done to distort a viscous material. While thermal conductivity, on the other hand, is a measure of heat transport efficiency. Many studies have been conducted on viscous dissipation and thermal conductivity due to their significance.

Effects of variable viscosity and dependent thermal conductivity on free convection flow along a vertical flat plate with heat conduction are significant from the different views. Researcher gets interest in the technology and process for their purpose. Sarker and Alam [1] studied the effects of variable viscosity and thermal conductivity on MHD natural convection flow along a vertical flat plate. Alam et al. [2]

considered the Effect of pressure stress work and viscous dissipation in natural convection flow along a vertical flat plate with heat conduction. Alim et al. [3] investigated the Joule heating effect on the coupling of conduction with MHD free convection flow from a vertical flat plate. Rahman et al. [4] presented the effects of temperature dependent thermal conductivity on MHD free convection flow along a vertical flat plate with heat conduction. Alim et al. [5] studied the combined effect of viscous dissipation & Joule heating on the coupling of conduction & free convection along a vertical flat plate. Molla et al. [6] considered the Natural convection flow along a vertical wavy surface temperature in presence of heat generation. Islam et al. [7] presented the effects of temperature dependent thermal conductivity on natural convection flow along a vertical flat plate with heat generation. Kabir et al. [8] analyzed the effects of viscous dissipation on MHD natural convection flow along a vertical wavy surface. Viscous and Joule heating effects on MHD free convection flow with variable plate temperature is investigated by Hossain [9]. Palani & Kim [10] studied numerical study on vertical plate with variable viscosity and thermal conductivity.

In this work, an analytical solution for the variable viscosity and dependent thermal conductivity in natural convection flow over a vertical flat plate in the presence of heat conduction will be produced based on experimental analysis. The discretization of momentum and energy equations in terms of non-dimensional coordinates X and Y in order to express the equations in finite difference form by approximating functions and derivatives in terms of the central differences in both coordinate directions. The numerical simulations of these equations led to the development of a computer code for the current issue, which uses an efficient implicit finite-difference approach. The Crank-Nicolson scheme is what it's called. For various parameters such as variable viscosity, dependent thermal conductivity, heat generation,viscous dissipation and Prandtl's number, the outcomes data analysis has developed for velocity profile, temperature profile, local skin friction, local Nusselt number, average skin friction, and average Nusselt number.

II. mathematical Analysis

The unsteady flow of a viscous incompressible fluid across a semi-infinite vertical plate is considered here. As indicated in Fig: 1, the *X*-axis is taken vertically upward along the plate, and the *Y*-axis is picked perpendicular to the plate at the leading edge. The origin of the *X*-axis is assumed to lie at the plate's leading edge. Except for the fluid viscosity, which varies exponentially with fluid temperature, the thermal conductivity, which varies linearly with fluid temperature, and the density variation in the body force term in the momentum equation, where the Bossiness approximation is used, all fluid physical properties are assumed to be constant.

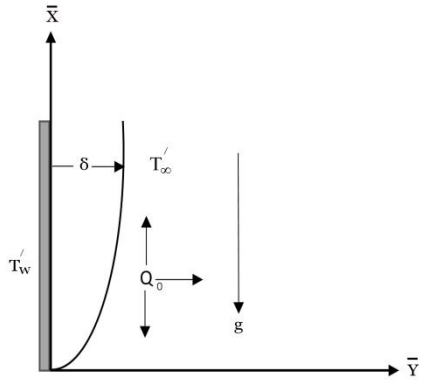

Fig:1 Plate Configuration

The mathematical statement of the basic conservation laws of mass, momentum and energy for the steady viscous incompressible and electrically conducting flow, after simplifying we have

$$\frac{\partial \bar{U}}{\partial \bar{X}}+\frac{\partial \bar{V}}{\partial \bar{Y}}=0 \tag{1}$$

$$\frac{\partial \bar{U}}{\partial t'}+\bar{U}\frac{\partial \bar{U}}{\partial \bar{X}}+\bar{V}\frac{\partial \bar{U}}{\partial \bar{Y}}=\frac{1}{\rho}\frac{\partial}{\partial \bar{Y}}\left(\mu\frac{\partial \bar{U}}{\partial \bar{Y}}\right)+g\beta\left(T'-T'\infty\right) \tag{2}$$

$$\frac{\partial T'}{\partial t'}+\bar{U}\frac{\partial T'}{\partial \bar{X}}+\bar{V}\frac{\partial T'}{\partial \bar{Y}}=\frac{1}{\rho Cp}\frac{\partial}{\partial \bar{Y}}\left(k\frac{\partial T'}{\partial \bar{Y}}\right)+\frac{\mu}{\rho Cp}\left(\frac{\partial U}{\partial \bar{Y}}\right)^2+\frac{Q_0}{\rho Cp}\left(T'-T'_\infty\right) \tag{3}$$

Here, $\bar{U}$ and $\bar{V}$ are the velocity components along the $\bar{X}$ and $\bar{Y}$ axis respectively, t' is the time, T' is the temperature of the fluid in the boundary layer and T'_∞ is the fluid temperature far away from the plate , g is the acceleration due to gravity, κ is the thermal conductivity of the fluid, ρ is the density, Cp is the specific heat at constant pressure and μ is the variable dynamic co-efficient of viscosity of the fluid. The amount of heat generated or absorbed per unit volume is $Q_0(T-T_\infty)$, Q_0 being a constant, which may take either positive or negative. The source term represents the heat generation when $Q_0 > 0$ and the heat absorption when $Q_0 < 0$. $k(T')$ is the thermal conductivity of the fluid depending on the fluid temperature T', σ_0 is the electric conduction.

The initial and boundary conditions are

$$\begin{aligned} &t' \le 0: \ \bar{U}=0, \bar{V}=0, \quad T'=T'_w \text{ for all } Y \\ &t' > 0: \ \bar{U}=0, \bar{V}=0, \quad T'=T'_w \text{ at } Y=0 \\ &t' > 0: \ \bar{U}=0, T'=T'_\infty \text{ at } X=0 \\ &t' > 0: \ \bar{U}\to 0, \quad T'\to T'_\infty \text{ as } Y\to\infty \end{aligned} \tag{4}$$

On introducing the following non-dimensional quantities in equations (1) to (4), we have

$$X=\frac{\bar{X}}{L},\ Y=\frac{\bar{Y}}{L}Gr^{1/4},\ U=\frac{L\bar{U}}{\nu}Gr^{-1/2},\ V=\frac{\bar{V}L}{\nu}Gr^{-1/4},\ t=\frac{\nu t'}{L^2}Gr^{1/2}, \tag{5}$$
$$T=\frac{T'-T'_\infty}{T'_w-T'_\infty},\ Gr=\frac{g\beta L^3\left(T'_w-T'_\infty\right)}{\nu^2},\ \mathrm{Pr}=\frac{\mu_0 Cp}{k_0},\ \nu=\frac{\mu_0}{\rho}$$

Here L is the length of the plate, ν is the kinematic viscosity, Gr is the Grashof number, Pr is the Prandtl number. Out of many forms of variation of viscosity and thermal conductivity with dimensionless temperature T, which are available in the literature. The following forms are proposed by Stattery [11], Ockendon and Ockendon [12], Elbashbeshy and Ibrahim [13], Wilson and Duffy [14], and Seddeek and Abdelmegguid [15]

$$\frac{\mu}{\mu_0}=e^{-\lambda T} \tag{6}$$

$$\frac{k}{k_0}=1+\Upsilon T \tag{7}$$

Where λ and Υ denote the viscosity and thermal conductivity variation parameters respectively, depended on the nature of the fluid. Here μ_0 and k_0 are the viscosity and the thermal conductivity at temperature T'_w.

The magneto hydrodynamic field in the fluid is governed by the boundary layer equations, which in the non-dimensional form obtained by introducing the dimensionless variables described in (5), may be written the equation of continuity as

$$\frac{\partial\bar{U}}{\partial\bar{X}}+\frac{\partial\bar{V}}{\partial\bar{Y}}=0$$

$$\Rightarrow \frac{\partial(\frac{\upsilon}{L}Gr^{\frac{1}{2}}U)}{\partial(X\,L)}+\frac{\partial(\frac{\upsilon}{L}Gr^{\frac{1}{4}}V)}{\partial(\frac{Y\,L}{Gr^{\frac{1}{4}}})}=0$$

$$\therefore \frac{\partial U}{\partial X}+\frac{\partial V}{\partial Y}=0 \tag{8}$$

Now momentum equation (2) can be reduced by applying the non- dimensional transformation (5) and (6), we have

$$\frac{\partial \bar{U}}{\partial t'}+\bar{U}\frac{\partial \bar{U}}{\partial \bar{X}}+\bar{V}\frac{\partial \bar{U}}{\partial \bar{Y}}=\frac{1}{\rho}\frac{\partial}{\partial \bar{Y}}\left(\mu\frac{\partial \bar{U}}{\partial \bar{Y}}\right)+g\beta\left(T'-T'_{\infty}\right)$$

$$\Rightarrow \frac{\partial\left(\frac{\nu}{L}Gr^{\frac{1}{2}}U\right)}{\partial\left(\frac{tL^2}{\nu Gr^{\frac{1}{2}}}\right)}+\frac{\upsilon}{L}Gr^{\frac{1}{2}}U\frac{\partial(\frac{\upsilon}{L}Gr^{\frac{1}{2}}U)}{\partial(X\ L)}+\frac{\upsilon}{L}Gr^{\frac{1}{4}}V\frac{\partial(\frac{\upsilon}{L}Gr^{\frac{1}{2}}U)}{\partial(\frac{YL}{Gr^{\frac{1}{4}}})}$$

$$=\frac{1}{\rho}\frac{\partial}{\partial\left(\frac{YL}{Gr^{\frac{1}{4}}}\right)}\left(\mu_0 e^{-\lambda T}\frac{\partial}{\partial\left(\frac{YL}{Gr^{\frac{1}{4}}}\right)}\left(\frac{\upsilon}{L}Gr^{\frac{1}{2}}U\right)\right)+g\beta T\left(T'_w-T'_{\infty}\right) \tag{9}$$

$$\Rightarrow \frac{\partial U}{\partial t}+U\frac{\partial U}{\partial X}+V\frac{\partial U}{\partial Y}=\left[e^{-\lambda T}\frac{\partial^2 U}{\partial Y^2}-\lambda e^{-\lambda T}\frac{\partial T}{\partial Y}\frac{\partial U}{\partial Y}\right]+T$$

Again, the energy equation (3) can be reduced by the above similarity transformation (5) and (7), we have

$$\frac{\partial T'}{\partial t'}+\bar{U}\frac{\partial T'}{\partial \bar{X}}+\bar{V}\frac{\partial T'}{\partial \bar{Y}}=\frac{1}{\rho Cp}\frac{\partial}{\partial \bar{Y}}\left(k\frac{\partial T'}{\partial \bar{Y}}\right)+\frac{Q_0}{\rho Cp}\left(T'-T'_{\infty}\right)+\frac{\mu}{\rho Cp}\left(\frac{\partial \bar{U}}{\partial Y}\right)^2$$

$$\Rightarrow \frac{\partial\left\{T'_{\infty}+T\left(T'_w-T'_{\infty}\right)\right\}}{\partial\left(tL^2/\nu Gr^{1/2}\right)}+\frac{\nu U}{L}Gr^{1/2}\frac{\partial\left\{T'_{\infty}+T\left(T'_w-T'_{\infty}\right)\right\}}{\partial(XL)}+\frac{\nu V}{L}Gr^{1/4}\frac{\partial\left\{T'_{\infty}+T\left(T'_w-T'_{\infty}\right)\right\}}{\partial\left(YL/Gr^{1/4}\right)}$$

$$=\frac{1}{\rho Cp}\frac{\partial}{\partial\left(YL/Gr^{1/4}\right)}\left(k\frac{\partial\left\{T'_{\infty}+T\left(T'_w-T'_{\infty}\right)\right\}}{\partial\left(YL/Gr^{1/4}\right)}\right)+\frac{Q_0}{\rho Cp}\left(T'-T'_{\infty}\right)+\frac{\mu}{\rho Cp}\left(\frac{\partial\left(\frac{\nu UGr^{\frac{1}{2}}}{L}\right)}{\partial\left(\frac{YL}{Gr^{\frac{1}{4}}}\right)}\right)^2$$

$$\Rightarrow \frac{\partial T}{\partial t}+U\frac{\partial T}{\partial X}+V\frac{\partial T}{\partial Y}=\frac{1}{\Pr}\left\{(1+\Upsilon T)\frac{\partial^2 T}{\partial Y^2}+\Upsilon\left(\frac{\partial T}{\partial Y}\right)^2\right\}$$

$$+\frac{Q_0L^2}{\rho Cp\nu Gr^{1/2}}\frac{(T'-T'_\infty)}{(T'_w-T')}+\frac{\mu\nu Gr}{\rho CpL^2(T'_w-T'_\infty)}\left(\frac{\partial U}{\partial Y}\right)^2$$

$$\Rightarrow \frac{\partial T}{\partial t}+U\frac{\partial T}{\partial X}+V\frac{\partial T}{\partial Y}=\frac{1}{\Pr}\left[\Upsilon\left(\frac{\partial T}{\partial Y}\right)^2\right]+\frac{1}{\Pr}\left[(1+\Upsilon T)\frac{\partial^2 T}{\partial Y^2}\right]+QT+\frac{\mu g\beta L}{\rho Cp\nu}\left(\frac{\partial U}{\partial Y}\right)^2$$

$$\Rightarrow \frac{\partial T}{\partial t}+U\frac{\partial T}{\partial X}+V\frac{\partial T}{\partial Y}=\frac{1}{\Pr}\left[\Upsilon\left(\frac{\partial T}{\partial Y}\right)^2\right]+\frac{1}{\Pr}\left[(1+\Upsilon T)\frac{\partial^2 T}{\partial Y^2}\right]+QT+N\left(\frac{\partial U}{\partial Y}\right)^2 \qquad (10)$$

The corresponding initial condition and boundary condition in a dimensionless form are as follows

$$\begin{aligned} &t\le 0:\ U=0, V=0,\quad T=0 \text{ for all } Y\\ &t\rangle 0:\ U=0, V=0,\quad T=1 \text{ at } Y=0\\ &\quad U=0,\quad T=0 \text{ at } X=0\\ &\quad U\to 0,\quad T\to 0 \quad at\ Y\to\infty \end{aligned} \qquad (11)$$

Equations (8) to (11) with the boundary condition (11) describe the free convective unsteady laminar boundary layer flow with variable viscosity and thermal conductivity along an isothermal semi-infinite vertical plate.

Where, $\Pr=\mu_0 Cp/k_0$, the Prandtl's number, $Q=Q_0L^2/\mu C_P Gr^{1/2}$ is the heat generation parameter and $N=g\beta L/Cp$ is the viscous dissipation parameter.

The local shear stress in the plate is defined by

$$\tau_{\bar{X}}=\left(\mu\frac{\partial\bar{U}}{\partial\bar{Y}}\right)_{\bar{Y}=0} \qquad (12)$$

By introducing the non-dimensional quantities given in equations (5) -(6) in (12), we get non-dimensional form of local skin friction and it is given by

$$\tau_{\bar{X}}=\left(\mu\frac{\partial\bar{U}}{\partial\bar{Y}}\right)_{\bar{Y}=0}$$

$$\Rightarrow \tau_{(XL)}=\left[\mu_0 e^{-\lambda T}\frac{\partial\left(\frac{U\nu}{L}Gr^{\frac{1}{2}}\right)}{\partial\left(YLGr^{-\frac{1}{4}}\right)}\right]_{Y=0} \qquad (13)$$

$$\therefore \bar{\tau}_X=Gr^{\frac{3}{4}}e^{-\lambda}\left[\frac{\partial U}{\partial Y}\right]_{Y=0}\ [at\ Y=0, T=1]$$

The integration of equation (13) from $X=0$ to $X=1$ gives the average skin friction and it is given by

$$\bar{\tau} = e^{-\lambda} Gr^{\frac{3}{4}} \int_0^1 \left(\frac{\partial U}{\partial Y} \right)_{Y=0} dX \tag{14}$$

The local Nusselt number is defined by

$$Nu_{\bar{X}} = \frac{-L\left(k \frac{\partial T'}{\partial \bar{Y}} \right)_{\bar{Y}=0}}{k_0 \left(T'_w - T'_\infty \right)}$$

$$\Rightarrow Nu_{(XL)} = \frac{-L\left(k_0 \left(1+\Upsilon T\right) \frac{\partial \left\{ T\left(T'_w - T'_\infty\right) + T'_\infty \right\}}{\partial \left(YLGr^{-\frac{1}{4}} \right)} \right)_{Y=0}}{k_0 \left(T'_w - T'_\infty \right)}$$

$$\Rightarrow Gr^{-\frac{1}{4}} \left(T'_w - T'_\infty \right) Nu_{(XL)} = -\left(1+\Upsilon\right)\left(\frac{\partial T}{\partial Y} \right)_{Y=0} \quad \because Y=0, T=1$$

$$\Rightarrow \bar{N}u_X = -\left(1+\Upsilon\right)\left(\frac{\partial T}{\partial Y} \right)_{Y=0}$$

$$\therefore \bar{N}u_X = -\left(1+\Upsilon\right)\left(\frac{\partial T}{\partial Y} \right)_{Y=0} \tag{15}$$

The integration of equation (15) from $X=0$ to $X=1$ gives the average skin friction and it is given by

$$\therefore Nu_X = -\left(1+\Upsilon\right) \int_0^1 \left(\frac{\partial T}{\partial Y} \right)_{Y=0} dX \tag{16}$$

III. Numerical Techniques

The two-dimensional, non-linear, unsteady and coupled partial differential Equations (8) -(10) under the initial and boundary conditions in Equation (11) are solved using an implicit finite difference scheme of Crank-Nicol-son type which is fast convergent and unconditionally stable. The finite difference equation corresponding to Equations (8) to (10) are given by

$$\frac{\left[U^{k+1}_{i,j} - U^{k+1}_{i-1,j} + U^{k}_{i,j} - U^{k}_{i-1,j} + U^{k+1}_{i,j-1} - U^{k+1}_{i-1,j-1} + U^{k}_{i,j-1} - U^{k}_{i-1,j-1} \right]}{4\Delta X}$$

$$+ \frac{\left[V^{k+1}_{i,j} - V^{k+1}_{i,j-1} + V^{k}_{i,j} - V^{k}_{i,j-1} \right]}{2\Delta Y} = 0 \tag{17}$$

$$\frac{\left[U^{k+1}_{i,j} - U^{k+1}_{i,j} \right]}{2\Delta t} + U^{k}_{i,j} \frac{\left[U^{k+1}_{i,j} - U^{k+1}_{i-1,j} + U^{k}_{i,j} - U^{k}_{i-1,j} \right]}{2\Delta X} V^{k}_{i,j} \frac{\left[U^{k+1}_{i,j+1} - U^{k+1}_{i,j-1} + U^{k}_{i,j+1} - U^{k}_{i,j-1} \right]}{4\Delta Y}$$

$$= \frac{1}{2}\left[T_{i,j}^{k+1} + T_{i,j}^{k}\right] + e^{-\lambda}\left[\frac{T_{i,j}^{k+1} + T_{i,j}^{k}}{2}\right]\frac{\left[U_{i,j-1}^{k+1} - 2U_{i,j}^{k+1} + U_{i,j+1}^{k} + U_{i,j-1}^{k} - 2U_{i,j}^{k} + U_{i,j+1}^{k}\right]}{2(\Delta Y)^2}$$

$$+e^{-\lambda}\left[\frac{T_{i,j}^{k+1} + T_{i,j}^{k}}{2}\right]\frac{\left[U_{i,j-1}^{k+1} - 2U_{i,j}^{k+1} + U_{i,j+1}^{k} + U_{i,j-1}^{k} - 2U_{i,j}^{k} + U_{i,j+1}^{k}\right]}{2(\Delta Y)^2}$$

$$-\lambda e^{-\lambda}\left[\frac{T_{i,j}^{k+1} + T_{i,j}^{k}}{2}\right]\frac{\left[T_{i,j+1}^{k+1} - T_{i,j-1}^{k+1} + T_{i,j+1}^{k} - T_{i,j-1}^{k}\right]}{4\Delta Y}\frac{\left[U_{i,j+1}^{k+1} - U_{i,j-1}^{k+1} + U_{i,j+1}^{k} - U_{i,j-1}^{k}\right]}{4\Delta Y} \tag{18}$$

$$\left[\frac{T_{i,j}^{k+1} - T_{i,j}^{k}}{2\Delta t}\right] + U_{i,j}^{k}\frac{\left[T_{i,j}^{k+1} - T_{i-1,j}^{k+1} + T_{i,j}^{k} - T_{i-1,j}^{k}\right]}{2\Delta X} + V_{i,j}^{k}\frac{\left[T_{i,j-1}^{k+1} - T_{i,j-1}^{k+1} + T_{i,j+1}^{k} - T_{i,j-1}^{k}\right]}{4\Delta y}$$

$$= \frac{1+\gamma T_{i,j}^{k}}{\Pr}\frac{\left[T_{i,j-1}^{k+1} - 2T_{i,j}^{k+1} + T_{i,j+1}^{k} + T_{i,j-1}^{k} - 2T_{i,j}^{k} + T_{i,j+1}^{k}\right]}{2(\Delta Y)^2} + \frac{\gamma}{\Pr}\left[\frac{\left[T_{i,j+1}^{k+1} - T_{i,j-1}^{k+1} + T_{i,j+1}^{k} - T_{i,j-1}^{k}\right]}{4\Delta Y}\right]$$

$$+\frac{\left[U_{i,j}^{k+1} - U_{i,j-1}^{k+1} + U_{i,j}^{k} - U_{i,j-1}^{k}\right]}{2\Delta Y}\frac{\left[U_{i,j}^{k+1} - U_{i,j-1}^{k+1} + U_{i,j}^{k} - U_{i,j-1}^{k}\right]}{2\Delta Y}N + \frac{Q}{2}\left[T_{i,j}^{k+1} + T_{i,j}^{k}\right] \tag{19}$$

The region of integration is considered as a rectangle with sides X_{max}(=1) and Y_{max}(=10), where Y_{max} Corresponds to $Y=\infty$, which lies very well outside the momentum and energy boundary layers. The maximum of *Y*was chosen as zero to several position after some preliminary investigations so that the last two of the boundary conditions (11) are satisfied. Here, the subscript *i*-designates the grid point along the *U*-direction, *j*-along the *V*-direction and the superscript *k* along the *t*-index. During any one-time step, the coefficients $U_{i,j}^{k}$ and $V_{i,j}^{k}$ appearing in the difference equations are treated as constants. The values of *U, V* and *T* are known at all grid points at *t* = 0, from the initial conditions. The computations of *U, V* and *T* at time level $(k+1)$ using the values at previous time level are carried out as follows: the finite difference equation (18) at every internal nodal point on a particular *i*-level constitute a tridiagonal system of equations. Such a system of equations is solved by Thomas algorithm as described in Carnahan *et al*. [16]. Thus, the values of *T* are found at every nodal point for a particular *i*at $(k+1)^{th}$ time level. Using the values of *T* at $(k+1)^{th}$ time level in the equation (13), the values of Uat $(k+1)^{th}$ time level are found in a similar manner. Thus, the values of *T* and *U* are known on a particular *i*-level. Finally, the values of *V* are calculated explicitly using the equation (12) at every nodal point on a particular *i*-level at $(k+1)^{th}$ time level. This process is repeated for various *i*-levels. Thus the values of *T, U* and *V* are known, at all grid points in the rectangular region at $(k+1)^{th}$ time level.

After considering with few sets of mesh sizes, they have been fixed at the level $\Delta X = 0.05$, $\Delta Y = 0.25$, and the time step $\Delta t = 0.01$. In this case, spatial mesh size is reduced by 50% in one-direction then in both directions, and the results are compared. It is observed that, when mesh size is reduced by 50% in *X*-direction and *Y*-direction, the results differ in fourth decimal place. Hence the above-mentioned sizes have been considered as appropriate mesh size for calculations. Computations are carried out until the steady-state is reached. The steady-state solution is assumed to have been reached, when the absolute difference between the values of *U,* as well as temperature *T* at two consecutive time steps are less than 10^{-5} at all grid points. The local truncation error is $O(\Delta f^2 + \Delta F^2 + \Delta X)$ and it tends to zero as $\Delta t, \Delta X$ and ΔY tend to zero, which shows that the scheme is compatible. Also, the Crank-Nicolson type of implicit finite difference scheme is proved to be unconditionally stable for a natural convective flow

in which there is always a non-negative value of velocity U and a non-positive value of V. Thus, compatibility and stability ensure the implicit finite difference scheme is convergent.

IV. Results and Discussions

The direct microscopic exchange of kinetic energy of particles via the border between two systems is known as heat conduction, sometimes known as diffusion. Water is an excellent heat transfer fluid because of its large thermal capacity and low viscosity. Oil has a greater liquid temperature than water, therefore it's been a popular alternative for avoiding the problem of high pressure. Heat is transferred between the Earth's surface and the atmosphere by conduction, radiation, and convection.

Heat is transferred via convection when a heated fluid, such as air or water, is forced to flow away from the source of heat, carrying energy with it. Convection happens when hot air expands, becomes less dense, and rises above a heated surface. Because liquid metals have a low Prandtl's number, heat transmission through molecular thermal conduction is important not only in the near-wall layer, but also in the flow core, even in a fully developed turbulent flow.

The following ranges for λ, ϒand Prare considered in the present study are:
For air: $-0.7 \le \lambda \le 0$, $0 \le \Upsilon \le 6$, $\Pr = 0.733$
For water: $0 \le \lambda \le 0.6$, $0 \le \Upsilon \le 0.12$, $1 \le \Pr \le 7.00$

In order to check the accuracy of our computed values, we compare our results with the curves computed by Sarker and Alam [1] &Palani and Kim [10]. for various values of λ and $\Upsilon$for air (Pr= 0.733). These are plotted in Figs. 2(a), 2(b). Our results agree very well with those of Sarker and Alam [1] &Palani and Kim [10]. at the steady state.

During the initial period the following step changes in the wall temperature, the body force has not had sufficient time to generate and appropriate motion in the fluid. Hence the velocity components $U$and V both are negligible for small time t. During this initial transient regime, the heat transfer is dominated by pure heat conduction, and hence for constant viscosity and thermal conductivity. Equation (10) reduces to

$$\frac{\partial T}{\partial t} = \frac{1}{\Pr}\frac{\partial^2 T}{\partial Y^2}$$

Thus, for short times, it is noted that for a given Prandtl's number, magnetic parameter, the temperature profile is a function of time only and normal distance from the wall. Setting Pr= 1, the solutions of equation. (15) subject to the initial and boundary conditions given in local Nusellt number are

$$T = erfc\left(\frac{Y}{2\sqrt{t}}\right) \qquad (20)$$

Figures 3 to 14 shows that the variation of velocity and temperature at their transient, temporal maximum and steady state against the co-ordinate Y at the leading edge of the plate viz., X = 1.0 for variable viscosity, thermal conductivity, heat conduction variation parameters, viscous dissipation and Prandtl's numbers. The fluid velocity increases and reached its maximum value at very near to the wall (i.e., $0 \le Y \le 2$) and then decreases monotonically to zero as Y becomes large for all time t. It is also observed that the velocity and temperature increase with time t, reaches a temporal maximum and consequently it reaches the steady state.

Figures 3(a) and 3(b) shows that the variation of transient velocity and temperature profiles with area A for a fixed value of Υ = 1.00 in air (Pr = 0.733), N = 0.40 and Q = 0.50. The velocity of the fluid increases with time until a temporal maximum is reached and thereafter a moderate reduction is observed until the ultimate steady state is reached. It is observed that the time taken to reach the steady state decreases marginally with an increasing the viscosity variation parameter.

From figure 3(a), it is clear that velocity U at any vertical plane near to the plate increases as X increases (the viscosity of air decreases). But an opposite trend is observed at a certain distance from the wall. From figure 3(b), it is observed that the temperature of the fluid decreases as λ increases (the viscosity of air decreases).

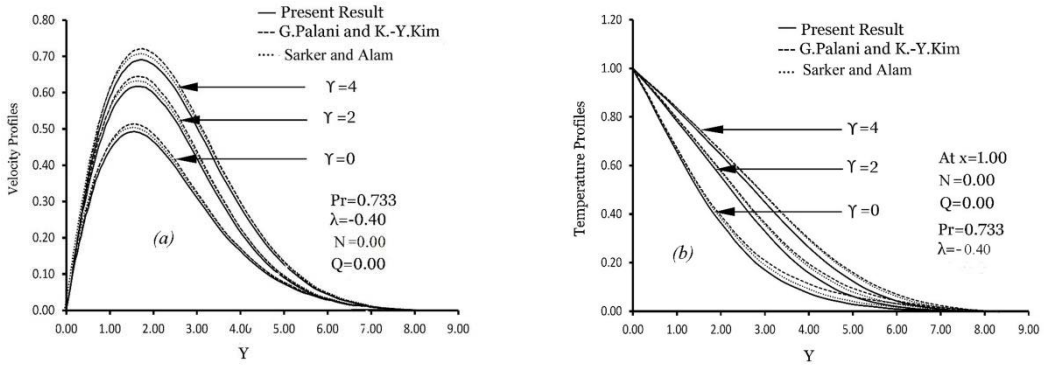

Figures 2(a) and 2(b): Variation of dimensionless velocity profiles and temperature profiles against dimensionless Y for different values of variable thermal conductivity parameter Υ with others fixed parameters.

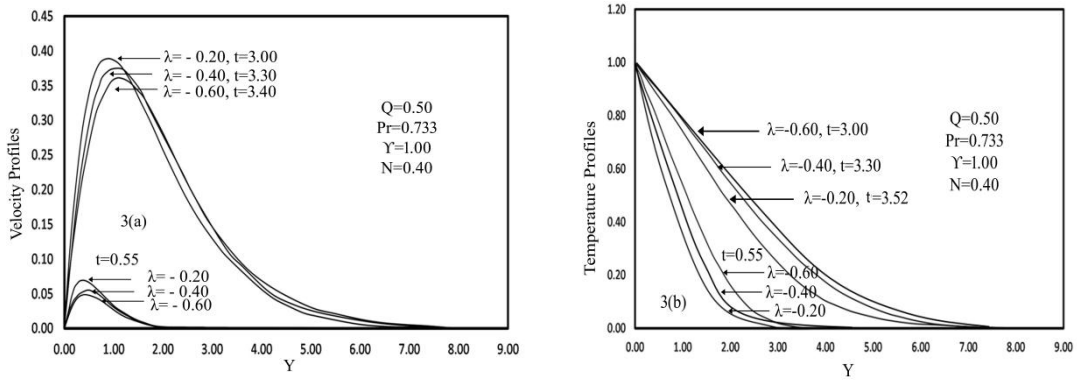

Figures 3(a) and 3(b): Variation of dimensionless velocity profiles and temperature profiles against dimensionless Y for different values of variable viscosity parameter λwith others fixed parameters.

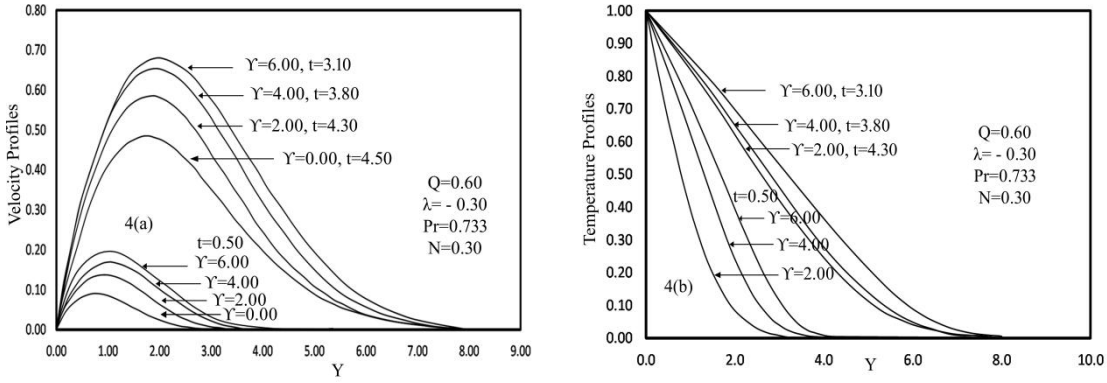

Figures 4(a) and 4(b): Variation of dimensionless velocity profiles and temperature profiles against dimensionless Y for different values of variable thermal conductivity parameter Υ with others fixed parameters.

The numerical values of the variation of transient velocity and temperature profiles with Υ for a fixed value of λ = - 0.30, Q = 0.60, N = 0.30 in air (Pr = 0.733) with the variation of thermal conductivity parameter Υ are shown graphically in figures 4(a) and 4(b). From these figures, it is observed that the velocity and temperature distribution in the fluid increases as Υincreases (thermal conductivity of air increases) for fixed value of λ, Q and Pr. It can also be noticed that with an increase in Υ, the rise in the magnitude of the velocity and temperature is significant, which implies that the volume flow rate increases with an increase in Υ. The effect of variation of thermal conductivity on velocity and temperature is more significant even in the initial transient period. Also, it is observed that the time to reach the temporal maximum and steady state decreases with increasing thermal conductivity parameter,Υ.

The numerical values of variation velocity and temperatures are calculated from equations (13) and (14) are depicted in the graphical form in the figures 5(a) and 5(b) for various values of N for fixed value of Q=0.60, Υ=0.90, λ=-0.40 in air (Pr=0.733).It is clearly noticed that the time taken to reach the temporal maximum and steady state decreases with an increasing the viscous dissipation parameter, N.It can be seen from figure 5(a) that an increase in the viscous dissipation parameter, N increases the velocity of the flow near the wall, because the viscosity of water decreases with an increase of the viscous dissipation parameter, N as seen in equation (6).Also, the maximum velocity gets very closer to the wall for higher values of N.This qualitative effect arises because, for the case of viscous dissipation (N> 0), the fluid is able to move more easily in a region close to the heated surface in association with the fact that the viscosity of the fluid with N> 0 is lower relative to the fluid with constant viscosity. This results in thinner velocity and thermal boundary layers.

It is observed that as Nincreases (the viscosity of water decreases), the velocity of the fluid particle increases only in the region $0 \leq y \leq 2$. From figure 5(b), it is noticed that the temperature profiles decrease with increasing N.This is in association with the fact that an increase in Nyields an increase in the peak velocity. The first effect increases the velocity of the fluid particle, due to the decrease in the viscosity and the second effect decreases the velocity of the fluid particle, due to the decrease in the temperature near the plate, the temperature $T$is high, consequently the first force will be dominant and the velocity Uincreases as N increases. On the other hand, the temperature $T$is low for far away from the plate, the second effect will be dominant and the velocity decreases as N increases. From the discussion, we notice that by neglecting the variation of fluid viscosity and thermal conductivity will introduce a substantial error.

Figures 6(a) and 6(b) shows that the variation of velocity and temperature for various values of Q for fixed value of N = 0.50, λ = - 0.20, Υ = 1.00in air (Pr= 0.733). It is observed that the time taken to reach the steady state decreases with the increasing value of Q. Also, it is observed that the temperature distribution of the fluid increases with the increasing value of Q.

The variation of transient velocity and temperature with variable viscosity for fixed values Pr = 7.00, N = 0.30, Q = 0.50 and Υ = 1.00 are shown in figures 7(a) and 7(b). It is observed that the time taken to reach the temporal maximum and steady state increases with the increasing value of variable viscosity parameter λ of the fluid. From the numerical results, we observe that the velocity profile increases with the increasing value of variable viscosity parameter λ.

The numerical values of variation of velocity and temperature profiles with N, for a fixed values of λ = 0.60, Υ = 0.50, Q = 0.40 for water (Pr = 7.00) are shown graphically in figures 8(a) and 8(b). From these figures, it is observed that time taken to reach the steady state is more when the viscous dissipation parameter N increases. Additionally, it is noticed that the velocity Increase as Nincreases near to the vertical plate. The temperature of the fluid increases as the viscous dissipation parameter N increases.

The variation of transient velocity and temperature with Prandtl's numbers for fixed values λ = 0.0, Υ = 0.80, N = 0.40 and Q = 0.60 are shown in figures 9(a) and 9(b). It is observed that the time taken to reach the temporal maximum and steady state increases with the increasing value of Prandtl's

number parameter Pr of the fluid. From the numerical results, we observe that the velocity profile increases with the increasing value of Prandtl's number parameter Pr. Larger Prandtl's number values give rise to thinner temperature profiles, because a larger Prandtl's number value means that the thermal diffusion from the wall is not prevailing, whereas the velocity diffusion extends far from the wall.

The variation of transient velocity and temperature with Heat Generation for fixed values of $\lambda = 0.50$, $\Upsilon = 0.70$, $N = 0.80$ and Pr = 7.00 are shown in figures 10(a) and 10(b). It is observed that the time taken to reach the temporal maximum and steady state increases with the increasing value of Heat Generation of the fluid. From the numerical results, we observe that the velocity profile decreases with the increasing value of Heat Generation.

The numerical values of the variation of transient velocity and temperature profiles with $\Upsilon$for a fixed value of $\lambda = 0.20$, $N = 0.40$, $Q = 0.60$ in water (Pr = 7.00) with the variation of thermal conductivity parameter Υ are shown graphically in figures 11(a) and 11(b). From these figures, it is observed that the velocity and temperature distribution in the fluid increases as Υincreases (thermal conductivity of air increases) for fixed value of λ, Q and Pr.

In figures 12(a) & 12(b), the effects of variation parameters and Pron local skin friction and local Nusselt number shown respectively for air (Pr=0.733).

The local skin-friction values are evaluated from equation (13) and plotted in figure. 12(a) as a function of the axial coordinate $\lambda$for air and water and selected values of the variation parameters λ and Υ.

The local skin-friction increases asλ increases. It is observed that local skin friction decreases with the increasing value of viscous variation parameter, λ. It is also observed that local wall shear stress increases with the increasing value of thermal conductivity parameter, Υ. An increase in the value of Prandtl's number, local skin friction is found to decrease.

In figures 13(a) & 13(b), the effects of variation parameters and Pron average skin friction and average Nusselt number shown respectively air (Pr=0.733). Average values of skin friction are calculated numerically from the equation (14) and are shown graphically in figure 13(a) for various values of viscosity and thermal conductivity parameters for air and water. It increases with time and reaches the steady state after a certain time lapse.

It is observed that average skin friction decreases with the increasing value of viscous parameter λ, viscous dissipation parameter and heat generation parameter Q. It is also observed that average wall shear stress increases with the increasing value of thermal conductivity parameter Υ. An increase in the value of Prandtl's number, average skin friction is found to decrease

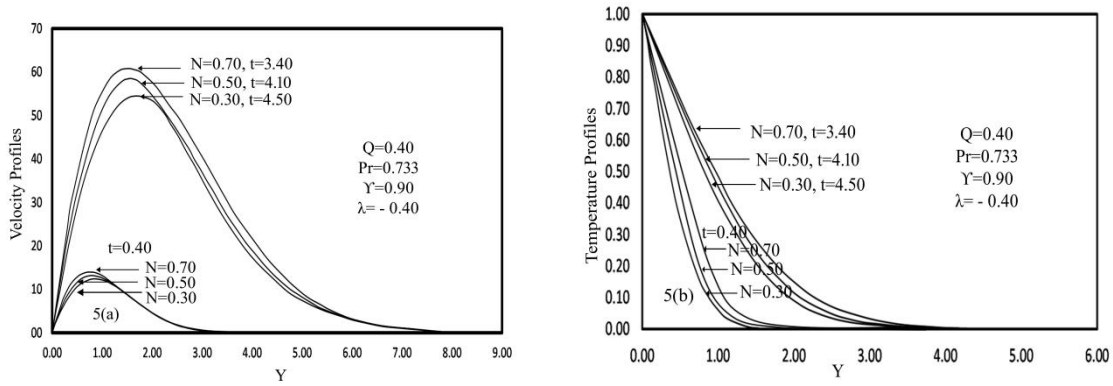

Figures 5(a) and 5(b): Variation of dimensionless velocity profiles and temperature profiles against dimensionless *Y* for different values of viscous dissipation parameter *N with* others fixed parameters.

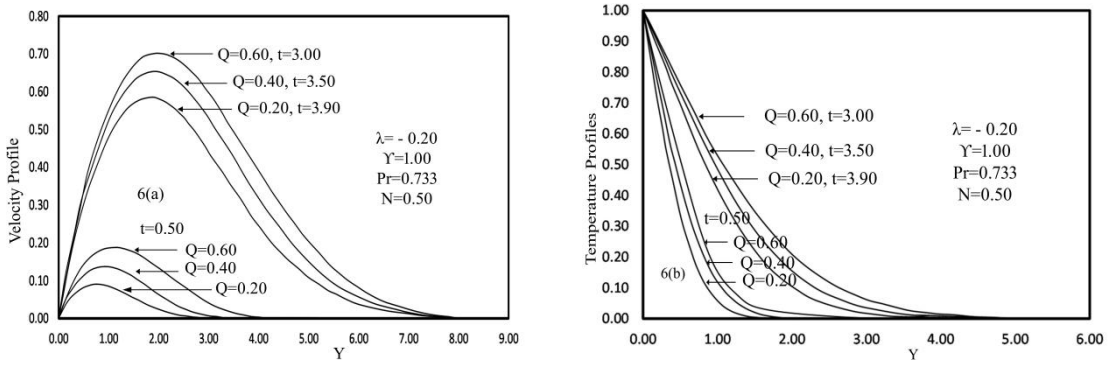

Figures 6(a) and 6(b): Variation of dimensionless velocity profiles and temperature profiles against dimensionless *Y* for different values of heat generation parameter *Q*with others fixed parameters.

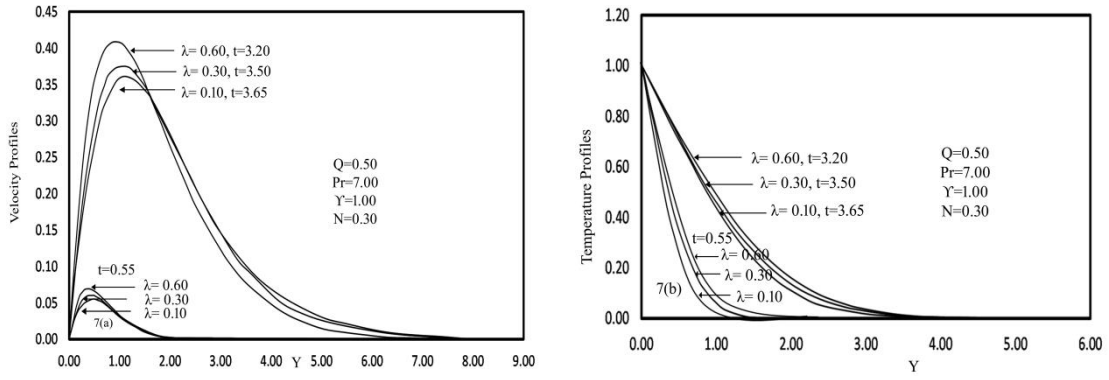

Figures 7(a) and 7(b): Variation of dimensionless velocity profiles and temperature profiles against dimensionless *Y* for different values of variable viscosity parameter*λ*with others fixed parameters.

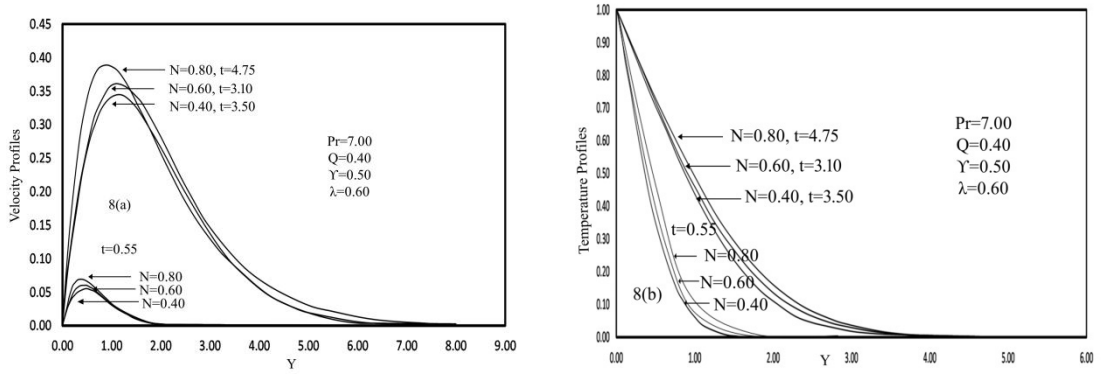

Figures 8(a) and 8(b): Variation of dimensionless velocity profiles and temperature profiles against dimensionless *Y* for different values of viscous dissipation parameter *Nwith* others fixed parameters.

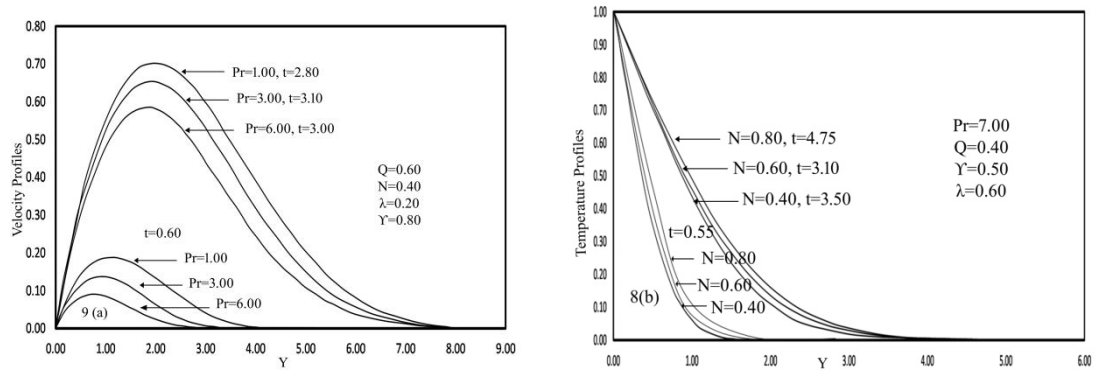

Figures 9(a) and 9(b): Variation of dimensionless velocity profiles and temperature profiles against dimensionless *Y* for different values of Prandtl's number parameter Pr with others fixed parameters.

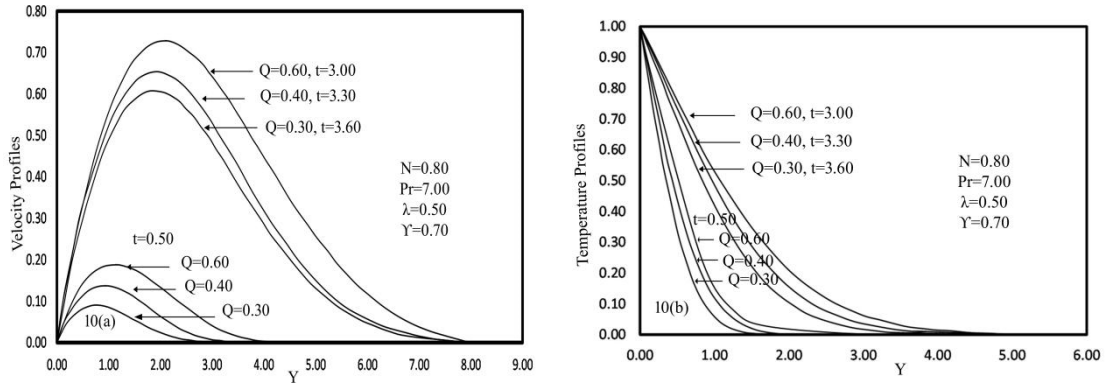

Figures 10(a) and 10(b): Variation of dimensionless velocity profiles and temperature profiles against dimensionless *Y* for different values of Heat generation *Q* with others fixed parameters.

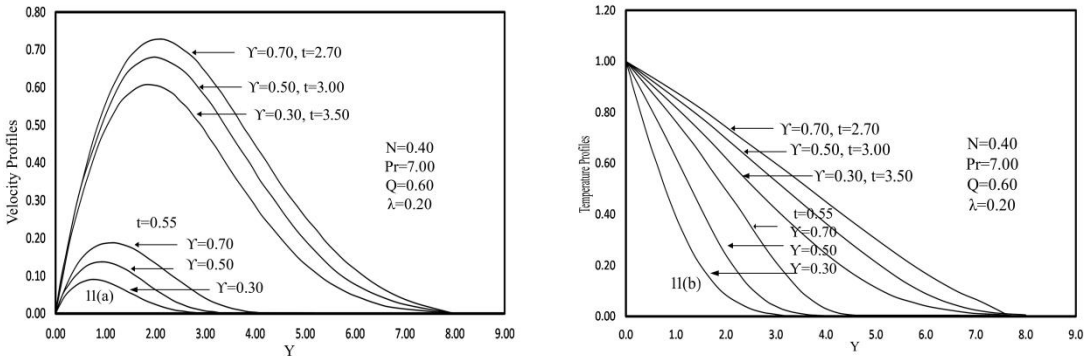

Figures 11(a) and 11(b): Variation of dimensionless velocity profiles and temperature profiles against dimensionless *Y* for different values of variable thermal conductivity parameter *ϒ* with others fixed parameters.

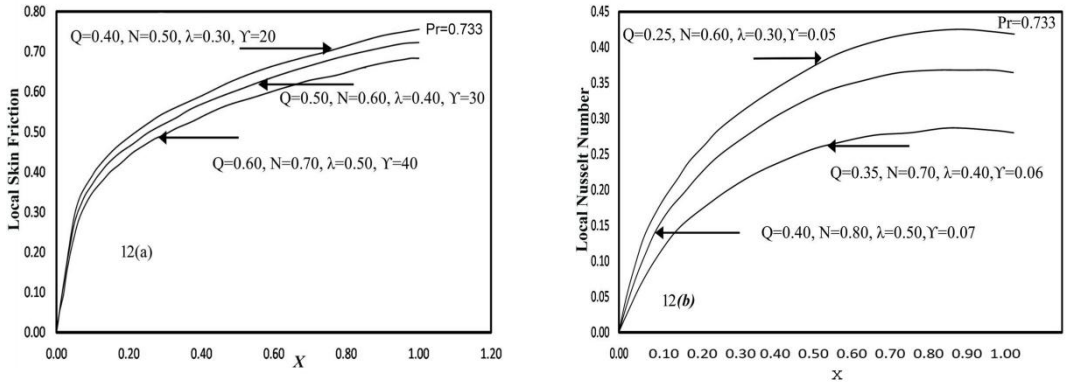

Figures 12(a) and 12(b): Variation of dimensionless local skin friction and local Nusselt number against dimensionless distance Xfor different values of *Q, N, λ*, *ϒ* and Pr=*0.733* at steady state condition.

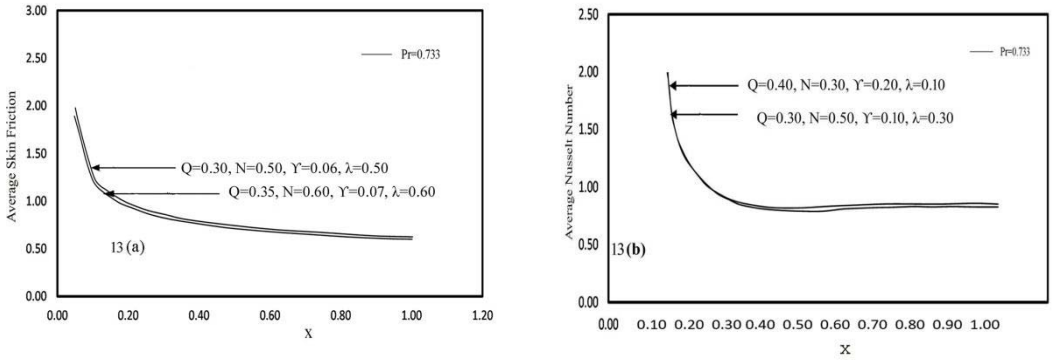

Figure 13(a) and 13(b): Variation of dimensionless average skin friction and average Nusselt number against dimensionless distance X for different values of *Q, N, λ*, *ϒ* and Pr=*0.733* at steady state condition.

In figures 14(a) & 14(b), the effects of variation parameters and Pron average skin friction and average Nusselt number shown respectively water (Pr = 6.00). An increase in the Prandtl's number lead to an increase in the average heat transfer rate, because increasing the Prandtl's number speeds up the spatial decay of the temperature in the flow field, yielding an increase in the rate of heat transfer and also same manner for heat generation parameter. It is also observed that average Nusselt's number decreases as *λ* , *ϒ* and *Q* increases.

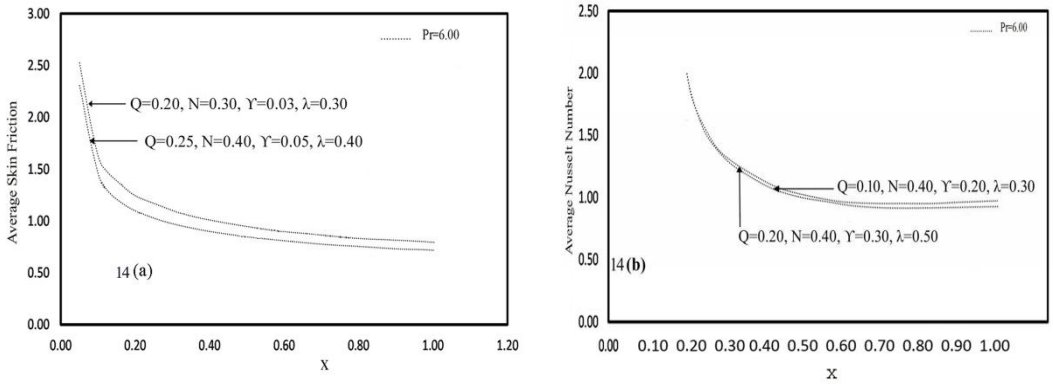

Figures 14(a) and 14(b): Variation of dimensionless average skin friction and average Nusselt number against dimensionless distance Xfor different values of *Q, N, λ*, *ϒ* and Pr=*6.00* at steady state condition.

Table-1: Comparing with Sarker & Alam [1] with our present work variation of dimensionless average skin friction against dimensionless distance x for different values of λ, Υ, N,Q and Pr at steady state condition.

X	Present	Sarker & Alam [1]	Present	Sarker & Alam [1]	Present	Sarker & Alam [1]
	$\overline{\tau}$	$\overline{\tau}$	$\overline{\tau}$	$\overline{\tau}$	$\overline{\tau}$	$\overline{\tau}$
0.000	0.000000	0.000000	0.000000	0.000000	0.000000	0.000000
0.100	0.937118	0.937229	0.698397	0.698541	0.172387	0.172542
0.200	1.311294	1.311428	0.951513	0.951672	0.246623	0.246775
0.300	1.478617	1.478761	1.012385	1.012542	0.281298	0.281431
0.400	1.539493	1.539658	1.057407	1.057552	0.337502	0.337653
0.500	1.542151	1.542269	1.058812	1.058966	0.354635	0.354781
0.600	1.545407	1.545538	1.059399	1.059541	0.365409	0.365541
0.700	1.548513	1.548669	1.059066	1.059219	0.367399	0.367543
0.800	1.551522	1.551649	1.065304	1.065432	0.369504	0.369651
0.900	1.563286	1.563431	1.075506	1.075654	0.376838	0.376976
1.000	1.567418	1.567568	1.079395	1.079543	0.378196	0.378341

Table-2: Comparing with Sarker & Alam [1] with our present work variation of dimensionless average Nusselt number against dimensionless distance x for different values of λ, Υ, N, Q and Pr at steady state condition

X	Present	Sarker & Alam [1]	Present	Sarker & Alam [1]	Present	Sarker & Alam [1]
	Nu_u	Nu_u	Nu_u	Nu_u	Nu_u	Nu_u
0.100	1.587904	1.588063	1.463888	1.464049	1.247011	1.247155
0.200	1.248188	1.248317	1.124058	1.124209	1.006288	1.006424
0.300	1.082271	1.082422	0.982792	0.982951	0.859009	0.859157
0.400	0.978511	0.978670	0.909585	0.909733	0.810115	0.810261
0.500	0.936025	0.936176	0.855047	0.855205	0.749695	0.749834
0.600	0.899734	0.899881	0.824974	0.825125	0.701701	0.701835
0.700	0.875897	0.876031	0.777153	0.777298	0.672307	0.672460
0.800	0.833955	0.834135	0.753689	0.753840	0.646032	0.646183
0.900	0.816622	0.816781	0.730170	0.730319	0.636939	0.637093
1.000	0.793282	0.793417	0.718861	0.719022	0.625912	0.626063

The comparison of the average skin friction and average Nusselt number between the present work and the work of Sarker & Alam [5] are presented in Table 1 and 2 respectively. We observe that the comparison is similar to the previous work. Our results are very similar to theirs.

V. Conclusion

The influence of changing viscosity and thermal conductivity on heat generation laminar natural convection boundary-layer flow along a vertical plate with pressure work is analyzed in this work. The thermal conductivity is assumed to be a linear function of temperature and the fluid viscosity is expected to fluctuate as an exponential function. An implicit Crank-Nicolson type finite difference approach is used to solve the dimensionless governing equations. Graphically, a comparison is drawn between the current numerical findings and previously published research. The agreement between the two parties is seen to be great. The present analysis has shown that:

(i) Reduced temperature and increased viscosity parameter λ cause a fluid to speed up. Whenever the viscosity variation parameter λ is large, the Nusselt number and skin friction are both raised, causing a boost in velocity near the wall.

(ii) As the thermal conductivity parameter Υ grows, the fluid velocity, fluid temperature, dimensionless wall velocity gradient, and dimensionless heat transfer rate from the plate to the fluid all rise.

(iii) Ignoring viscosity and thermal conductivity differences leads to considerable errors. Thus, to predict more precise results, viscosity and heat conductivity must be considered.

(iv) Increasing the viscous dissipation parameter N moderately raises the velocity profiles. Additionally, a higher temperature profile is observed with higher values of the viscous dissipation parameter.

(v) For both the velocity and temperature distributions, a rise in the heat generation parameter Q results in substantial improvements.

(vi) The local skin friction coefficient, the local Nusselt number, and the velocity distribution over the entire boundary layer all decrease, while the temperature distribution increases. This is because the temperature distribution is independent of the other variables (Q, N, λ, and Υ) that affect heat generation and dissipation, respectively.

References

[1] SreePradip Kumar Sarker and Alam M..M. “Effect of Variable Viscosity and Thermal Conductivity on MHD Natural Convection Flow along a Vertical Flat Plate”, Journal of Advances in Mathematics and Computer Science, Vol. 36, No. 3, pp. 58-71, 2021

[2] Alam M.M., Alim M. A., and Chowdhury M. M. K. “Effect of pressure stress work and viscous dissipation in natural convection flow along a vertical flat plate with heat conduction”, *Journal of Naval Architecture and Marine Engineering*, Vol. 3, No. 2, pp. 69-76, 2006.

[3] Alim M. A., Alam M. M. and Abdullah Al-Mamun “Joule heating effect on the coupling of conduction with magneto-hydrodynamic free convection flow from a vertical flat plate”, *Nonlinear Analysis: Modeling and Control,* Vol. 12, No. 3, pp. 307-316, 2007.

[4] Rahman M. M., Mamun A. A., Azim M.A. and Alim M.A. “Effects of temperature dependent thermal conductivity on MHD free convection flow along a vertical flat plate with heat conduction”, *Nonlinear Analysis: Modeling and Control,* Vol. 13, No. 4, pp. 513-524, 2008.

[5] Alim M. A., Alam M. M., Abdullah Al-Mamun and Belal Hossain “The combined effect of viscous dissipation & Joule heating on the coupling of conduction & free convection along a vertical flat plate”, *International Communications in Heat and Mass Transfer*, Vol. 35(3) pp.338-346, 2008.

[6] Molla M.M., Hossain M.A. and Yao L.S. “Natural convection flow along a vertical wavy surface temperature in presence of heat generation/absorption”, *Int. J. Thermal Science*, Vol.43, pp.157-163, 2004.

[7] Safiqul Islam, M. A. Alim, M. M. A. Sarker and A. F. M. Khodadad Khan, “Effects of

temperature dependent thermal conductivity on natural convection flow along a vertical flat plate with heat generation", *Journal of Naval Architecture and Marine Engineering*, JNAME, Vol. 9, No. 2, pp. 113-122, Dec, 2012.

[8] Kabir K. H., Alim M. A. and Andallah L. S. "Effects of viscous dissipation on MHD natural convection flow along a vertical wavy surface", Journal of *Theoretical and Applied Physics, a Springer Open Journal*, Vol. 7, No. 31, pp. 1-8, 22, June 2013.

[9] Hossain M. A. "Viscous and Joule heating effects on MHD free convection flow with variable plate temperature", *Int. J. Heat and Mass Transfer*, Vol.35 (2), pp.3485-3487, 1992.

[10] Palani and Kim, "Numerical study on vertical plate with variable viscosity and thermal conductivity", Springer-Verlag, Vol. 80, pp. 711-725, 2009.

[11] Stattery, J.C Momentum, Energy and Mass Transfer in Continua. McGraw Hill, New York. 1972.

[12] Ockendon H and Ockendon J.R. "Variable-viscosity flows in heated and cooled channels", J. Fluid Mech, Vol. 83(1), pp. 177-190, 1977

[13] Elbashbeshy E.M.A. and Ibrahim F.N. "Steady free convection flow with variable viscosity and thermal diffusivity along a vertical plate", J. Phys. D Appl. Phys, Vol. 26(12), pp. 237-2143, 1993

[14] Wilson S. and Duffy B. "On lubrication with comparable viscus and inertia forces",Quarterly Journal of Mechanics and Applied Mathematics, Vol.51, Pt.1 pp.105-124, 1998.

[15] Seddeek M.A. and Abdelmeguid M.S. "Effects of radiation and thermal diffusivity on heat transfer over a stretching surface with variable heat flux", Phys. Lett. A, Vol. 348(3-6), pp. 172-179,2006.

[16] Carnahan B., Luther H.A., Wilkes J.O. : Applied Numerical Methods. Wiley, New York (1969)